Thermal Design of Astrobee Perching Arm

In-Won Park[1], Trey Smith[2] and John F. Love[2]

***Abstract*— This paper presents the thermal design of actuators in the perching arm of Astrobee robot that will operate inside the International Space Station (ISS) in starting 2019. Since the crew's safety is of the utmost importance on the ISS, all materials used in the Astrobee robot should meet the touch temperature requirements according to the ISS safety standards to protect crew from skin burns by controlling the exposure temperature. The Astrobee perching arm consists of 2-DOF arm servo motors and 1-DOF gripper DC motor, which are capable of overheating in the stalled condition. Thermal properties of two types of actuators are verified by monitoring the touch temperature in worst-case operations with no thermal protection. Then, the proper thermal protection designs have been conducted and installed to guarantee the safety in all conditions.**

I. INTRODUCTION

The Intelligent Robotics Group at NASA Ames Research Center is building a free-flying robot, Astrobee, which will be operated inside the International Space Station (ISS) in starting 2019 to perform a variety of intravehicular activities. Astrobee is expected to support autonomous operations, remote operation by ground controllers, and human-robot interaction with crew members [1]–[5]. Fig. 1 shows the flight unit of Astrobee docking on the charging station on the top of micro-gravity simulating surface.

A. Perching Arm

As a part of the Astrobee robotic system, a compliant, detachable perching arm is being developed to support long duration tasks. This arm will grasp ISS handrails to hold its position without using propulsion or navigation to minimize power consumption. It will also support Astrobee robots grasping each other to enable future research related to satellite servicing.

Fig. 2 shows the flight unit of 3-DOF Astrobee perching arm consists of payload lever, arm proximal joint, arm distal joint, and gripper, where the design of structure and avionics are presented in [6]. The payload levers support quick release/locking mechanism to the Astrobee payload volume. The crew does not require additional tool to install the arm to the Astrobee payload bay, where the magnets act as stop and holder for the levers. In addition, the lever is operable by one hand, which requires 5 N of force applied at the lever tip.

[1]Author is with SGT Inc. within the Intelligent Robotics Group, NASA Ames Research Center, Moffett Field, CA 94035, USA in.w.park@nasa.gov

[2]Authors are with NASA Ames Research Center, Moffett Field, CA 94035, USA trey.smith@nasa.gov, john.f.love@nasa.gov

Fig. 1. Astrobee docking on the station on the top of micro-gravity simulating surface.

The 2-DOF arm joints are used to stow the gripper inside of the outer structure during flight so that it is not exposed to collision hazard while stowed. When the arm is successfully perched on the ISS handrail, it can also operate as a pan-tilt module for a camera attached on the opposite side of the robot to support remote monitoring operations [7]. The 1-DOF gripper uses torsional springs for joint flexion and an actuated tendon for extension. This allows gripping force to be maintained even with the motor turned off. It also allows external forces to open the gripper by overcoming spring torques, rather than having to back-drive the motor. Furthermore, independent flexion torques at the proximal and distal joints provide passive compliance to the shape of the grasped object; the perching procedure is thus robust to positioning errors with respect to the handrail.

The 2-DOF arm motors and 1-DOF gripper motor are capable of overheating itself due to operating near stall conditions or failure in firmware update. Thus, these actuators must ensure that either active of passive thermal controls are designed and developed to pass the ISS safety standards for touch temperature requirements. This paper presents the passive thermal control used in 2-DOF arm motors and the active thermal control used in 1-DOF arm motor.

This paper is organized as follows. Section II describes the thermal requirement for touch temperature in the ISS. Section III presents the experimental results of arm motor and gripper motor tested in the worst-case operations without any thermal protection to understand the thermal properties of each actuator. Section IV explains the proposed thermal

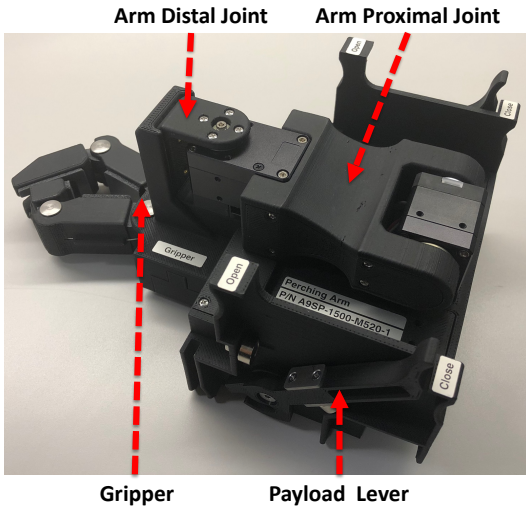

Fig. 2. Flight unit of 3-DOF Astrobee perching arm.

TABLE I

HOT TOUCH TEMPERATURE LIMITS FOR ASTROBEE MATERIALS.

Material	Inverse Thermal Inertia $[(k\rho c)^{-1/2}]$	Incidental 1 Second [°C]	Incidental 10 Second [°C]	Infinite Contact [°C]
Steel	3.26	73	52	46
Aluminum	4.91	75	51	47
Glass	28.8	96	64	57
Ultem	56	122	76	68

control strategy and concluding remarks follow in Section V.

II. THERMAL REQUIREMENT

The perching arm shall comply with ISS safety standards for touch temperature requirements to protect crew from skin damage by controlling the exposure to pain. The maximum touch temperature depends on the thermal conductivity, which is calculated from the thermal inertia of material and initial temperature, and skin contact time. Assuming that the material is homogeneous, Table I presents the touch temperature limits for material used in the Astrobee robot, where k, ρ, and c represent thermal conductivity, density, and specific heat, respectively. The temperature values in Table I are determined by linear interpolation, which are set in SSP 50005F ISS Flight Crew Integration Standard document.

In addition to the touch temperature limits, any component that is capable of overheating itself shall have either active or passive thermal controls, where the active thermal control need to be single fault tolerant (require two independent methods). Any component that uses active thermal control should be verified by disabling one of the thermal controls and executing a worst-case operation to maximize the exterior temperature. Once the first control prevents exceeding the touch temperature limit, then the test should be repeated while the other thermal control is disabled.

Arm motors for proximal and distal joints and gripper motor are the potential heat sources as shown in Fig. 2. The arm motor (Dynamixel XH430-W210) has aluminum

TABLE II

PARAMETER SETUP OF ARM MOTORS AND CURRENT CONSUMPTION IN STALL CONDITION.

Test Condition	PWM Limit [%]	Temperature Limit [°C]	Current Consumption [A]
(1)	100	80	1.58
(2)	80	80	1.12
(3)	70	80	0.90
(4)	50	80	0.64
(5)	50	80	0.65
(6)	50	100	0.60

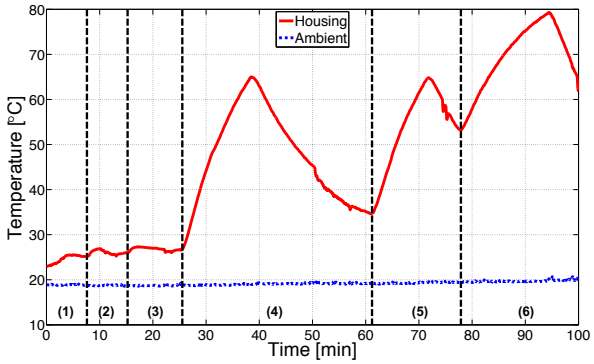

Fig. 3. Surface temperature of arm motor in stall condition.

case, which could act as a better heat sink, but it is exposed to the crew and is cooled primarily by radiation to the ISS environment. An overheating event may occur when the arm motor goes into a prolonged stall, when the PWM limit is set incorrectly or not handled properly, or when the maximum internal temperature limit fails. Unfortunately, the COTS firmware is involved in the last two cases, where any firmware involved becomes safety critical due to a bug in the COTS firmware or a radiation event in the ISS. The gripper motor (Pololu Micro Gearmotor) is enclosed in Ultem and not exposed to the crew, but the touch temperature should be monitored while actuating the motor near the stall condition.

III. RESULTS WITHOUT THERMAL PROTECTION

This section describes the experimental results of arm motor and gripper motor to understand the thermal properties. Both motors are tested in the worst-case operations without any thermal protection to maximize the metal housing temperature.

A. Arm Motor - Dynamixel XH430

In the test setup, the thermocouples are placed on the top of external aluminum surface and the arm link to measure the touch temperature, and one on the table to measure ambient temperature. At the end of arm link, 60 g of dummy mass has been added to create a resistance torque and to simulate the inertia of the Astrobee during a panning motion aboard the ISS. In addition to the thermocouples, the perching arm controller board has monitored both internal motor temperature provided by the COTS firmware and current consumption by the current sensor.

In the normal operating condition, the internal and external temperature are reached to 40°C and 31°C, respectively, and 0.19 A of current is consumed after 47 minutes when the temperature is reached near equilibrium while the motor is continuously moving. If one assumes the maximum ISS internal temperature is 30 °C, the temperature can increase up to 17 °C because the touch temperature of aluminum for infinite contact is 47 °C as shown in Table. I. The ambient temperature at the start of the test is 19 °C meaning that as long as the temperature stays below 36 °C, the touch temperature limit would not be reached. Since the external temperature measured from thermocouple was 31°C, the arm motor has been passed the normal operating conditions. During the test, heat has been transferred to the arm link, but the highest temperature was the aluminum surface of arm motor.

Table. II indicates the parameter setups for various test conditions and the corresponding current consumption in the stall condition. Fig. 3 shows the temperature of external motor surface measured from the thermocouple. The arm joint is clamped to the table and the initial test is ran with the internal temperature limit set to default, which is 80°C, and the maximum PWM limit in the COTS firmware. The current reading has increased rapidly to a max of about 1.58 A, but fluctuates about 1.5 $\pm$ 0.08 A, which is above the stall current 1.3 A. After 10 seconds, the current reading has returned to a low value of about 0.09 A showing that the arm motor has stopped. As shown in Table. II and Fig. 3, the COTS firmware automatically disable the motor power until the value of PWM limit has been changed to 50 %.

When value of PWM limit has been set to 50 %, the external aluminum surface temperature kept increasing until the internal temperature limit of COTS firmware has reached. When the internal temperature limit has set to 80 °C, the difference between the internal temperature provided by the COTS firmware and the measured external temperature was 15.0 °C and 15.2 °C in test conditions 4 and 5, respectively. However, the difference has been increased to 20.7 °C when the temperature limit has been increased to 100 °C. Since the resulting temperature values are higher than the touch temperature limits for aluminum in Table I, it would be necessary to design the thermal control that does not rely on the firmware.

B. Gripper Motor - Pololu Micro Gearmotor

Fig. 4 shows the current consumption of gripper motor in the normal operating condition. It consumes the peak maximum current of 0.62 A and 0.50 A each time for actuating the tendon to open the gripper by overcoming torsional spring forces. It would require about 0.2 A to hold the gripper open, which is well below the stall current of 0.8 A.

Fig. 5 shows the extreme temperature increase on the gripper motor surface when the over-current above the stall current is applied to the motor. In this condition, the motor has ceased to function and the surface temperature has been increased above the touch temperature limit. Even though

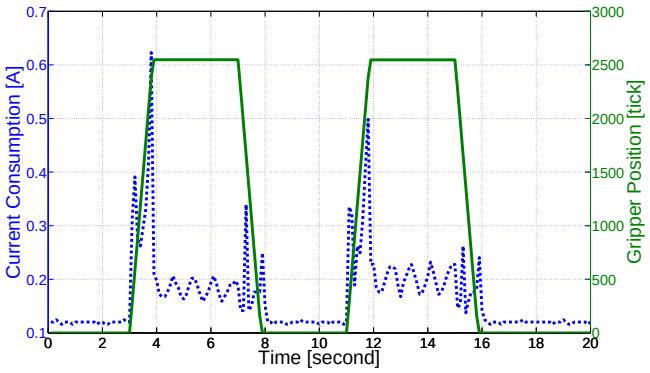

Fig. 4. Current consumption of gripper motor in normal condition.

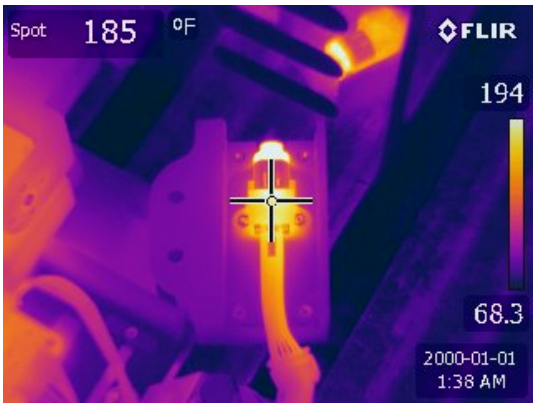

Fig. 5. Surface temperature of gripper motor in over-current condition.

the gripper motor is enclosed in Ultem and not exposed to the crew, the motor would require the thermal control to prevent overcurrent indicative of locked up, stalled, or jammed condition.

IV. Thermal Design

This section introduces the thermal design of arm motor and gripper motor that guarantees safety in all conditions.

A. Arm Motor - Bimetallic Thermostat Selection

The perching arm motors for panning and tilting joints are exposed to the crew and are cooled primarily by radiation to the ISS environment, but also conduction through Ultem 9085 links back to the Astrobee structure. The motors do not exceed the touch temperature limit in normal operations, but in some cases, the temperature on the metal motor housing has gone up above this limit in stall conditions as shown in Fig. 3. Both arm motors provide the load information on force exerted by arm and stop applying the torque if resistance detected. In addition, the internal temperature sensors cuts off the power if it exceeds the preset temperature limit. However, these two methods depend on the firmware for safety, where a radiation event may cause the motor to misbehave in the ISS.

In order to guarantee the passive thermal safety in all conditions, a bimetallic thermostat is placed on the metal motor housing, which monitors the surface temperature and

cuts off the power if it exceeds the preset temperature. When the bimetallic thermostat is heated, the internal stress causes the bimetallic disc to reverse its curvature with a snap-action to open the electrical contacts of motor power. When it is below the preset temperature, the bimetallic disc relieves the internal stress and returns its curvature to normal operation condition. The specifications of bimetallic thermostat are given in terms of operating temperature (T), differential (D), and error tolerance (E). Based on these specifications, the expected two behaviors of thermostat are as follows:

- When closed, the thermostat opens at nominal temperature, T
- When opened, the thermostat closes at nominal temperature, $T - D$

where both of these temperature threshold values have error bars of $\pm E$.

The following extra parameters are considered for analysis:

- Let K be the temperature of the hottest point on the metal motor housing that is exposed to inadvertent crew touch.
- Let L be the temperature of the thermostat contact point on the metal motor housing.
- Let M be the temperature of the thermostat.
- Let $Y = K - L$. The size of arm motor is small and its rate of heating is limited. Thus, the entire metal motor housing should have fairly consistent temperature equalized through thermal conduction. The thermostat contact point may actually be hotter than any point exposed to crew contact, because exposure to the cabin provides a cooling effect. We have conservatively bounded, $Y = \pm 3°\text{C}$.
- Let $Z = L - M$. The thermostat has low thermal inertia and is in direct metal-to-metal contact with the motor housing. Since the motor is the heat source, the thermostat should be cooler than the motor housing. We have conservatively assumed, $0 < Z < 3°\text{C}$.
- Let S be the threshold value for a touch temperature hazard on the metal motor housing exposed to crew. Per the ISS safety requirement shown in Table I, we are using the threshold for 1 second inadvertent touch on aluminum, $S = 75°\text{C}$.
- Let A be the maximum ambient temperature in the ISS cabin. We have assumed, $A = 30°\text{C}$.
- Let N be the hottest K can get during the nominal operations. The worst-case observed ΔT was approximately 17°C. This ΔT has been added to the worst-case ambient temperature to get $N = 47°\text{C}$.

The key safety requirement is that the thermostat shall open when there is a touch temperature hazard, which is defined as follows:

$$T + E + Y + Z < S \tag{1}$$

where $T + E$ represents the highest thermostat temperature when thermostat open. Using the maximum values in the possible ranges for Y and Z, (1) is reduced as follows:

$$T < 69°\text{C} - E \tag{2}$$

In order to enable the nominal operation of perching arm, the thermostat shall not open during nominal operations, which is defined as follows:

$$T - E > N - Y - Z \tag{3}$$

where $T - E$ represents the lowest thermostat temperature when thermostat is opened and N represents the highest temperature during nominal operations. Using the minimum values in the possible ranges for Y and Z, (3) is reduced as follows:

$$T > 50°\text{C} + E \tag{4}$$

Ideally, in the unlikely event that the thermostat ever trips, the thermostat shall close after an extended period of non-operation to restore the functionality of perching arm, which is defined as follows:

$$T - D - E > A \tag{5}$$

where $T - D - E$ represents the lowest thermostat temperature when thermostat is closed and A represents the highest thermostat temperature after extended non-operation. Using the maximum ambient temperature in the ISS cabin, (5) is reduced as follows:

$$T > 30°\text{C} + D + E \tag{6}$$

Having plenty of design margin is more important with regard to the top end of the range, because if there is any issue with the bottom end of the range, there is an option to mitigate it with the operations rule on the duty cycle of arm operations. This leads to the following rules for selecting the optimal thermostat:

- Prefer the differential D and error tolerance E to be as small as possible.
- Choose the lowest T that still satisfies both constraints (4) and (6).
- Verify constraint (2) is satisfied.

Based on the datasheet, Klixon M1130110122 has been selected and it has been placed on the bottom surface of each arm motor as shown in Fig. 6. This thermostat opens at 130°F ($\approx 54.4°\text{C}$) and closes back to normal operation at 110°F ($\approx 43.3°\text{C}$) with the tolerance of $\pm 2.8°\text{C}$. During installation, thermal conductive adhesive (3M TC-2810) is applied on the face of thermostat that contacts the motor to fill the possible gap. Since this design does not counting on the firmware of arm motors for thermal safety, the maximum internal temperature limit of arm motor is set high that the firmware cutoff will not disrupt the nominal operations.

B. Gripper Motor - Current Limiter Circuit

Gripper DC motor is encased and air gap insulated in Ultem 9085, not touchable by the crew. However, as shown in Fig. 5, the metal motor housing reaches to 85°C ($\approx 185°\text{F}$) in the over-current condition without any thermal protection. The controller board is capable of monitoring the current

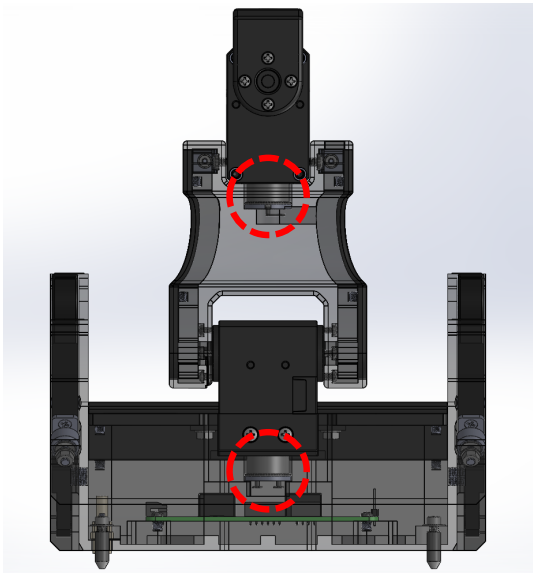

(a) Location of Bimetallic Thermostat

(b) Snapshot of Bimetallic Thermostat

Fig. 6. Passive thermal design on arm motors.

that is being applied and stop applying the torque if the load is higher than preset threshold. However, as mentioned in Section II, any firmware involved in thermal control becomes safety critical.

For the gripper motor, an active thermal control approach is used that requires to enforce touch temperature limits are single fault tolerant. The first control approach is verified by monitoring the touch temperature while actuating the gripper motor near the maximum current level in the normal operations. As shown in Fig. 4, the peak maximum current was below the stall current. The second control approach is verified by obstructing motion in a worst-case stall condition. In order to prevent over-current due to locked up, stalled, or jammed condition, a current limiter circuit is designed, where the block diagram of the current limiter circuit is shown in Fig. 7.

In the current limiter circuit, the SR flip flop (74LVC2G02) is placed in between the micro-controller (dsPIC33E) and the motor driver (MC33926) to disable the motor driver when the over-current occurs. When the perching arm is powered on, the micro-controller sends the state of '1' to the SR flop flop such that the 'EN' of motor driver becomes '1'. In order to avoid the unknown state, the micro-controller sends the state of '0' when the motor driver is enabled.

During the operation, the analog voltage that represents the current feedback of the motor driver (MC33926) is compared to the reference voltage, which is set to 90 % of the stall current. When the feedback voltage is greater than this reference voltage, the comparator triggers the multi-vibrator (SN74LVC1G123) that sends a short rising edge pulse to the SR flip flop. This makes the 'EN' of motor driver to become '0' and disable the motor driver completely. The mico-controller monitors the status of motor driver and is capable of enabling the motor driver back on by sending the state of '1' to the SR flop flop.

V. CONCLUSIONS

With the proposed thermal design, there is no way for the exposed surface of Astrobee perching arm to exceed above the touch temperature limits, without relying on firmware controls.

ACKNOWLEDGMENT

We would like to thank the ISS Payloads Office, the JSC Flight Operations Directorate, ISS Avionics and Software, the Advanced Exploration Systems program, the ISS SPHERES team, and the Astrobee team for their collaboration.

This research was supported by the NASA Game Changing Development Program (NASA Space Technology Mission Directorate) and the ISS SPHERES Facility (NASA Human Exploration and Operations Mission Directorate).

REFERENCES

[1] M. Bualat, J.Barlow, T. Fong, C. Provencher, T. Smith and A. Zuniga, "Astrobee: Developing a free-flying robot for the international space station," in *Proc. AIAA Space 2015*, Aug. 2015, pp. 1–10.

[2] J. Yoo, I.-W. Park, V. To, J. Lum and T. Smith, "Avionics and perching systems of free-flying robots for the international space station," in *Proc. IEEE Int. Symp. Sys. Eng.*, Sept. 2015.

[3] T. Smith, J. Barlow, M. Bualat, T. Fong, C. Provencher, H. Sanchez, E. Smith and the Astrobee Team, "Astrobee: A new platform for free-flying robotics on the international space station," in *Proc. Int. Symp. Artificial Int. Robot. Autom. Space*, Jun. 2016.

[4] B. Coltin, J. Fusco, Z. Moratto, O. Alexandrov and R. Nakamura, "Localization from visual landmarks on a free-flying robot," in *Proc. IEEE/RSJ Int. Conf. Intell. Robot. Syst.*, Oct. 2016, pp. 4377–4382.

[5] Evan Ackerman, IEEE Spectrum, *How NASA's Astrobee robot is bringing useful autonomy to the ISS*, Available: http://spectrum.ieee.org/automaton/robotics/space-robots/how-nasa-astrobee-robot-is-bringing-useful-autonomy-to-the-iss

[6] I.-W. Park, T. Smith, S. W. Wong, P. Piacenza and M. Ciocarlie, in *Proc. IEEE Int. Conf. Adv. Int. Mech.*, Jul. 2017, pp. 1135–1141.

[7] D.-H. Lee, B. Coltin, T. Morse, I.-W. Park, L. Fluckiger and T. Smith, "Handrail detection and pose estimation for a free-flying robot," *Int. J. Adv. Robot. Sys.*, vol. 15, no. 1, pp. 1–12, 2018.

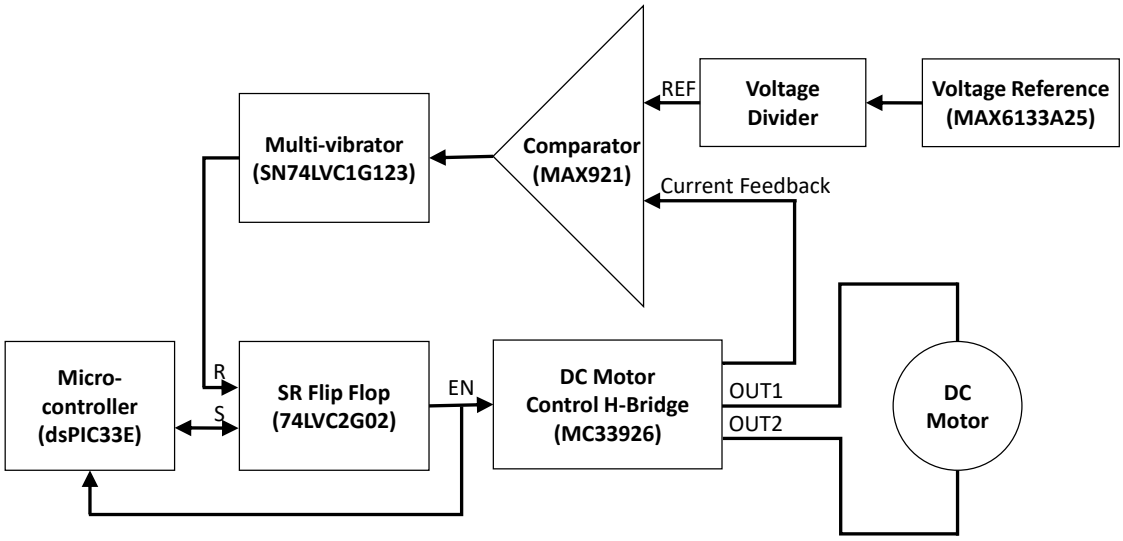

Fig. 7. Active thermal design of gripper motor using the current limiter circuit.